ORIGINAL ARTICLE

Vibration suppression of aeroengine casing during milling

Liang Guo[1] · Fan Yang[1] · Tian Li[2] · Ming Zhou[1] · Junlei Tang[3]

Abstract

The casing is a basal body part for assembling other parts in an aeroengine, but its weak rigidity seriously affects machining accuracy and production efficiency. Therefore, it is very important to improve this rigidity of the part during processing. An aeroengine combustor casing is used to study the vibration law and suppression method of a casing milling process through a combination of simulations and physical experiments in this paper. First, the milling vibration law of a Rolls-Royce aeroengine combustor casing is analysed through mechanical analysis and machining vibration detection, and then a simulation experiment environment based on physical experiment verification is established. Second, based on a virtual experimental platform, the free mode and constraint mode of the casing without auxiliary support, multipoint rigid auxiliary support, and flexible surface auxiliary support schemes are analysed. Subsequently, to determine the optimal support pressure for different types of casing parts produced on-site, after analysing the common size range of the casing, 3^4 and 4^3 full-factor simulation experiments are performed, and the influence of each factor on the change in vibration is summarised. Finally, a static load experiment is used to verify that the clamping scheme of the flexible surface auxiliary support can improve the radial rigidity of the casing. Through the experimental research in this paper, the results show that the error between the simulation experiment results and the physical experiment is basically kept within 20%, and the established virtual experiment is reliable. At the same time, based on the simulation data in this paper, the function expressions of vibration deformation and support pressure, milling force, case thickness, and casing diameter are fitted, and the R-square reaches 91.2%. This empirical formula provides theoretical support for the selection of optimal support air pressure and the prediction of vibration and deformation.

Keywords Milling vibration · Vibration suppression · Aeroengine · Casing · Finite element analysis

1 Introduction

Aero engines are typical knowledge-intensive and technology-intensive high-tech products. They play a leading role in national defence construction, the national economy, and scientific and technological development. Their design and manufacturing capabilities largely represent the technological level and competitiveness of a country's manufacturing industry. The aeroengine casing is a base part for assembling the other parts in an aeroengine, and it is also an important load-bearing component that requires high processing quality. Due to the functional requirements of the casing, the materials are all high-temperature materials, and the structure is complicated. The thinnest part can reach 2 mm. The large size and high accuracy requirements can lead to poor processability, but the material removal rates can reach $80 \sim 90\%$. To complete such complex machining requirements, milling is primarily used. However, during processing, the rigidity of the system to be processed, consisting of parts and fixtures, is weaker than that of the tool system, so the dynamic stability of the system to be processed cannot be guaranteed. By combining modal analysis and the structural optimization of the system to be processed, the system's natural frequency can be increased while its stiffness is increased to improve the dynamic stability of the system to be processed.

Research on the vibration suppression of thin-walled rotating bodies is mainly divided into theoretical research and new tooling design. Wan et al. [1] proposed a new method to improve the stability of thin-walled parts by applying stress

✉ Liang Guo
  gl@swpu.edu.cn

1 School of Mechatronic Engineering, Southwest Petroleum University, No. 8, Xindu Avenue, Chengdu 610500, China

2 AECC Chengdu Engine Co., Ltd, Chengdu 610503, China

3 School of Chemistry and Chemical Engineering, Southwest Petroleum University, Chengdu 610500, China

during milling. Wan et al. [2] designed a new spindle system and integrated a new electromagnetic actuator to suppress machining vibration. Yue et al. [3] summarised the current status of machining chatter prediction, identification, and control and summarised the use of neural networks, support vector machines, and the Hilbert-Huang algorithm to realise machining vibration detection. Liu et al. [4] concluded that an unequal spacing arrangement has the effect of damping vibration by studying the arrangement of ribs. Bolar et al. [5] conducted 81 full-factor experiments with reasonable cutting parameters to analyse the influence of process parameters on the surface quality of parts. Fang et al. [6] established a vibration equation based on shell theory and solved the analytical method of free vibration. Wang et al. [7] analysed and found the optimal combination of fixture and cutting parameters through the combination of particle swarm optimization and the finite element method. Wang et al. [8] applied the Hamiltonian principle and combined the Rayleigh-Ritz method to establish mechanical equations. It was concluded that restrained damping can effectively restrain the vibration transmission of thin-walled cylindrical shells. Zhang et al. [9] established a kinematic model of a system and a calculation model between the contact force fixture components and further proposed optimizing the clamping force to maintain the stability of the system. Tan et al. [10] used a finite element method to analyse the vibration of a stiffened cylindrical shell model. The results show that the arrangement and structure of the ribs have a large effect on the vibration of the thin-walled shell only at medium and high frequencies where the structural wavelength and rib spacing are equivalent. Munoa et al. [11] analysed different flutter suppression techniques and identified corresponding industrial applications. Wang et al. [12] established a thin-walled cylindrical shell dynamic model based on the LOVE shell theory and compared the effects of the modal damping ratio and excitation force on the response. Kolluru et al. [13] and D. Axint studied the coupled dynamic response of tools and workpieces in open and closed geometries and explained the coupling between tools and thin-walled parts and the impact dynamics during machining. By et al. [14] proposed an analytical solution model for the static deformation prediction of thin plates with weak stiffness. Starting from the fixture body, Siebenaler et al. [15] discussed the influence of its flexibility on the deformation of the workpiece.

In terms of tooling for practical applications, Fei et al. [16] proposed providing a support element on a back of the machining tool and moving it at the same time as the tool to achieve vibration suppression. Do et al. [17] proposed an optimal positioning method relative to the fixture system based on the part geometry extracted from a CAD model. Sallese et al. [18] introduced a fixture that actively suppresses flutter using low-frequency excitation and verified its effectiveness through physical experiments. Qin et al. [19] established a finite element

model of the clamping layout from the perspective of the clamping deformation impact of the fixture on the machining accuracy and surface quality. Ma et al. [20, 21] used a new dynamic analysis model to determine the impact of damping factors on the dynamic response during processing and verified the accuracy of the model using a magnetorheological fluid fixture. Wang et al. [22] used a low melting point alloy with a melting point of 70° and used its low shrinkage to clamp thin-walled parts. Wan et al. [23] analysed the effect of fixture layout on the dynamic response of thin-wall multi-framed workpiece(TMW) during machining. Jiang et al. [24] proposed a new type of magnetorheological fluid auxiliary support fixture for the weak rigidity of thin-walled aviation parts and analysed the influence of magnetorheological fluid volume and magnetic field strength on machining vibration. Yang et al. [25] proposed using the resistance of machining vibration to the workpiece to suppress the vibration, and experiments showed that the milling stability was increased by more than 2 times. Kolluru et al. [26–28] proposed a surface damping solution consisting of a flexible thin layer plus discrete mass viscoelastic layers and proposed a new torsion spring pretensioned articulation device for forced vibration. Zeng et al. [29] suppressed the machining vibration of the workpiece by designing a reasonable fixture arrangement scheme. It can be seen from the above literature that although there are a large number of experimental and theoretical analyses of thin-walled parts or thin-walled revolving parts in existing research, there are few studies on aeroengine combustor casings. Although some studies have addressed casing parts, few studies have been conducted on the suppression of milling vibration and vibration deformation prediction from the perspective of the support method and the parameters of the casing itself.

A Rolls-Royce aeroengine combustor casing from a certain aeroengine manufacturing company in Chengdu is studied in this paper, and ABAQUS software is used for finite element analysis and physical experiment verification. A finite element analysis model is constructed, and free modal and constrained modal analyses are performed. The natural frequency of the clamping system is tested by hammering. Finally, the modal-based steady-state dynamics in ABAQUS linear perturbation are used to analyse the simulation processing, and a regression model of vibration deformation prediction with reference value is The subsequent sections are arranged as follows: Section 1 analyses the causes of vibration during the milling process of the casing. Section 2 analyses the processing system based on simulations and physical experiments. Section 3 uses ABAQUS software to analyse the harmonic response of the processing system. Section 4 verifies the effect of structural rigidity improvement through static load experiments. Section 5 concludes the paper and presents future study directions.
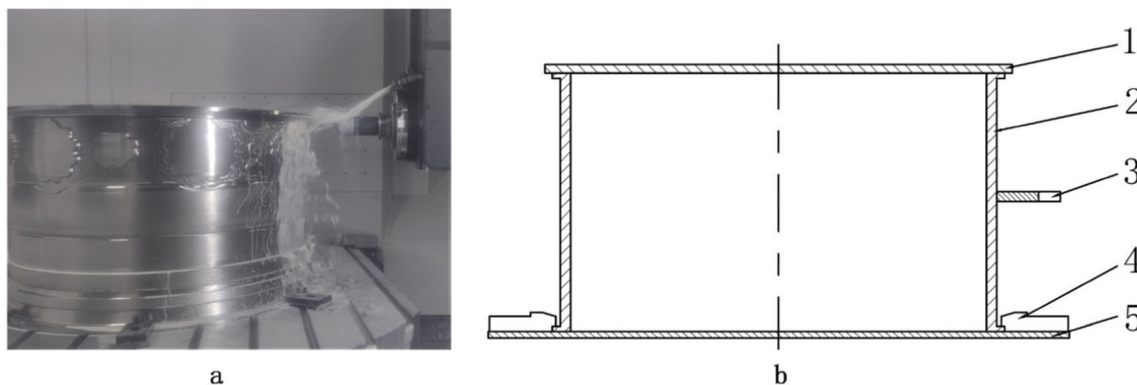
Fig. 1 Schematic diagram of the milling process with the conventional unsupported fixture. 1. Top clamping plate 2. Casing part 3. Milling cutter 4. Clamp 5. Base

2 Vibration analysis of casing milling

In the aeroengine manufacturing company, the 5-axis CNC turning and milling machining center is used in the turning-milling of the internal wall reinforcement ribs, external wall multi-island features, and cylindrical surface of Rolls-Royce aeroengine combustor casing parts [30]. This article mainly analyses the deformation of the casing caused by the milling force when milling the outer wall. As shown in Fig. 1 1-a is the processing site, and 1-b is the simplified processing diagram. When the casing is milled using a conventional non-internal support fixture, the clamp is specifically placed on the machining center table and fixed, and the lower mounting edge of the casing part is restrained on the concrete base by the clamp. The clamp directly restricts the axial movement of the casing, and at the same time, the circumferential and radial movements that the casing may produce during milling are limited by the friction between the clamp and the mounting edge.

Under the abovementioned processing environment, during the high-speed milling of the casing parts, the dynamic milling force $f(x,s)$ is generated due to the periodic contact and separation of the milling cutter and the surface to be processed. The milling force can be decomposed into the combination of the three directions of the x, y, and z axes (i.e. axial, radial, and circumferential). Among them, the casing parts are restrained by the clamp and the top clamping plate to enhance the ability of the component to resist stretching and bending while reducing axial deformation. The dynamic milling force in the circumferential direction continuously acts on the point of force and the direction is unchanged, so no obvious vibration deformation will occur in the circumferential direction. In the radial direction, the force point of the dynamic milling force $f(x,s)$ on the part of the radial component force moves with the milling cutter trajectory and always points to the axis. In view of the fact that the casing parts are not supported in the radial direction, when the milling force is applied to the surface of the casing, the force point will be elastically deformed instantaneously and the direction will be inward. The subsequent restoring force of the part will force the deformation area of the part to rebound and move outward, so it will produce more obvious vibration in the radial direction, as shown in Fig. 2.

In addition to the radial unsupported deformation during the milling of the casing, vibration analysis, and actual detection of the unsupported milling processing status of a Rolls-Royce aeroengine combustor casing processed on-site is used to analyse whether resonance is also one of the factors that cause deformation. The experimental results are shown in

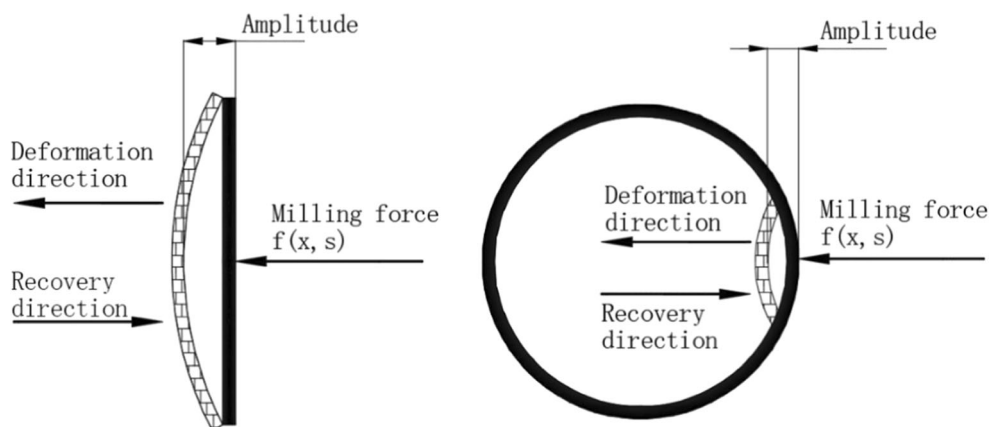Fig. 2 Milling force radial force component
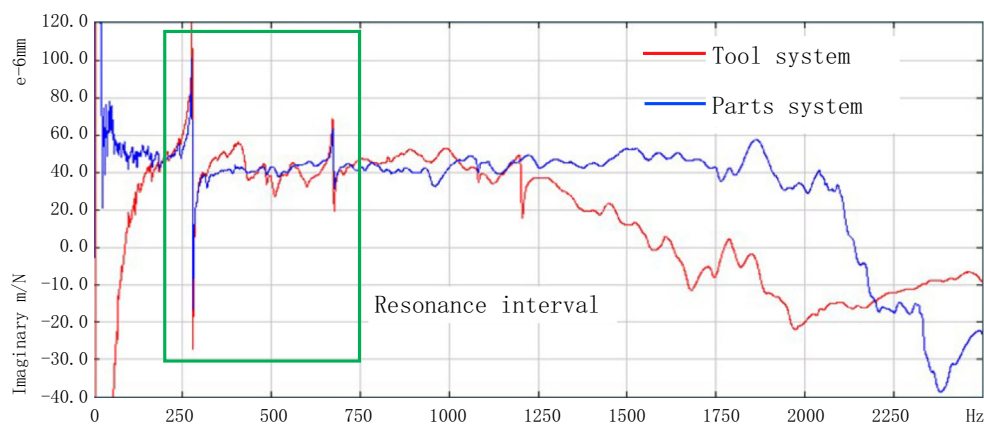
Fig. 3 Vibration analysis test
results

Fig. 3. It can be seen in the figure that the system to be proc-
essed and the tool system including parts are susceptible to
resonance between 250 and 650 Hz. Therefore, optimizing the
structure of the system to be processed to avoid the resonance
interval is very important for the vibration suppression of the
processing.

After analysing the milling process of a Rolls-Royce
aeroengine combustor casing and the vibration state during
processing, there are two reasons for the excessive vibration
of the casing processing: (1) the natural frequency of the sys-
tem to be processed and the machine tool processing system
are close which causes resonance; (2) the thin wall casing is a
weakly rigid component and poor rigidity results in poor re-
sistance to deformation. Therefore, the vibration suppression
of the processing of the casing parts mainly starts from the
optimization and improvement of the support fixture system,
changes the natural frequency of the system to be processed,
avoids the resonance interval, and improves the system rigid-
ity. In the next chapter of this article, the structural perfor-
mance will be optimised from the perspective of the free

modal of the casing parts and the constrained modal of the
system to be processed.

3 Modal analysis based on simulation and physical experiments

There are many small features on the surface of the casing
parts in actual production and processing, such as rounds,
chamfers, and small holes. However, such small features have
little effect on the dynamic performance of the casing part
structure, and it is extremely inconvenient to build a finite
element model. Therefore, taking Fig. 4-a Rolls-Royce
aeroengine combustor casing as an example, the actual model
is simplified to retain only the outline and dimensions when
drawing the 3D model of the casing part in UG. The simplified
model is shown in Fig. 4-b, and the model size parameters are
shown in Table 1. Finally, the modal analysis module in the
linear perturbation of the finite element analysis software

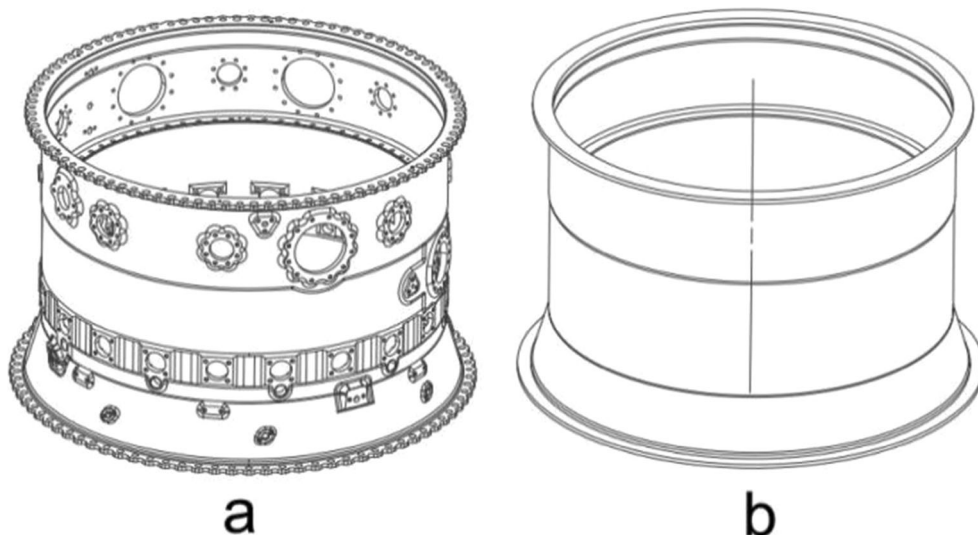**Fig. 4** Simplified combustion
chamber model

Table 1 Casing parameters

Parameter	Inside diameter mm	Height mm	Case thickness mm	Young's modulus Gpa	Poisson's ratio	Density g/cm3
Value	800	600	5	199.9	0.3	8.24

ABAQUS was used to perform modal analysis on the part, including free modal and constrained modal.

3.1 Free modal analysis

The purpose of a modal analysis is to determine the vibration characteristics of a structure or machine component, that is, to analyse the natural frequency and mode shape of the structure or component. Among them, the results of the free modal analysis can show the strength of the vibration of each part of the structure and the weak area of resistance to vibration, providing the necessary theoretical basis for the later research and design of the support scheme.

In the free modal analysis of the casing parts, there are no constraints on the 6 degrees of freedom of the parts. Therefore, in the modal analysis results, the natural frequencies of the first six orders are close to 0 Hz, and the mode shapes of the remaining orders are shown in Fig. 5. Through simulation

analysis, it can be found that the natural frequencies of order 7–10 of the parts are 51.025 Hz, 53.177 Hz, 79.214 Hz, and 83.965 Hz. At the same time, it can be seen from the 7 to 10 order mode shapes that the deformation trend of parts is mostly radial deformation, especially concentrated at the mounting edges at the upper and lower ends of the part. Therefore, the structural characteristics of the casing parts must be improved from the perspective of radial support.

3.2 Constrained modal analysis

3.2.1 Constrained modal analysis based on finite element

After a free modal analysis of the model, it is planned to design an auxiliary support milling and clamping system for the casing parts. Two support schemes are shown in Fig. 6. Option 2 is a conventional multi-point rigid support, and option 3 is a new type of flexible surface contact support
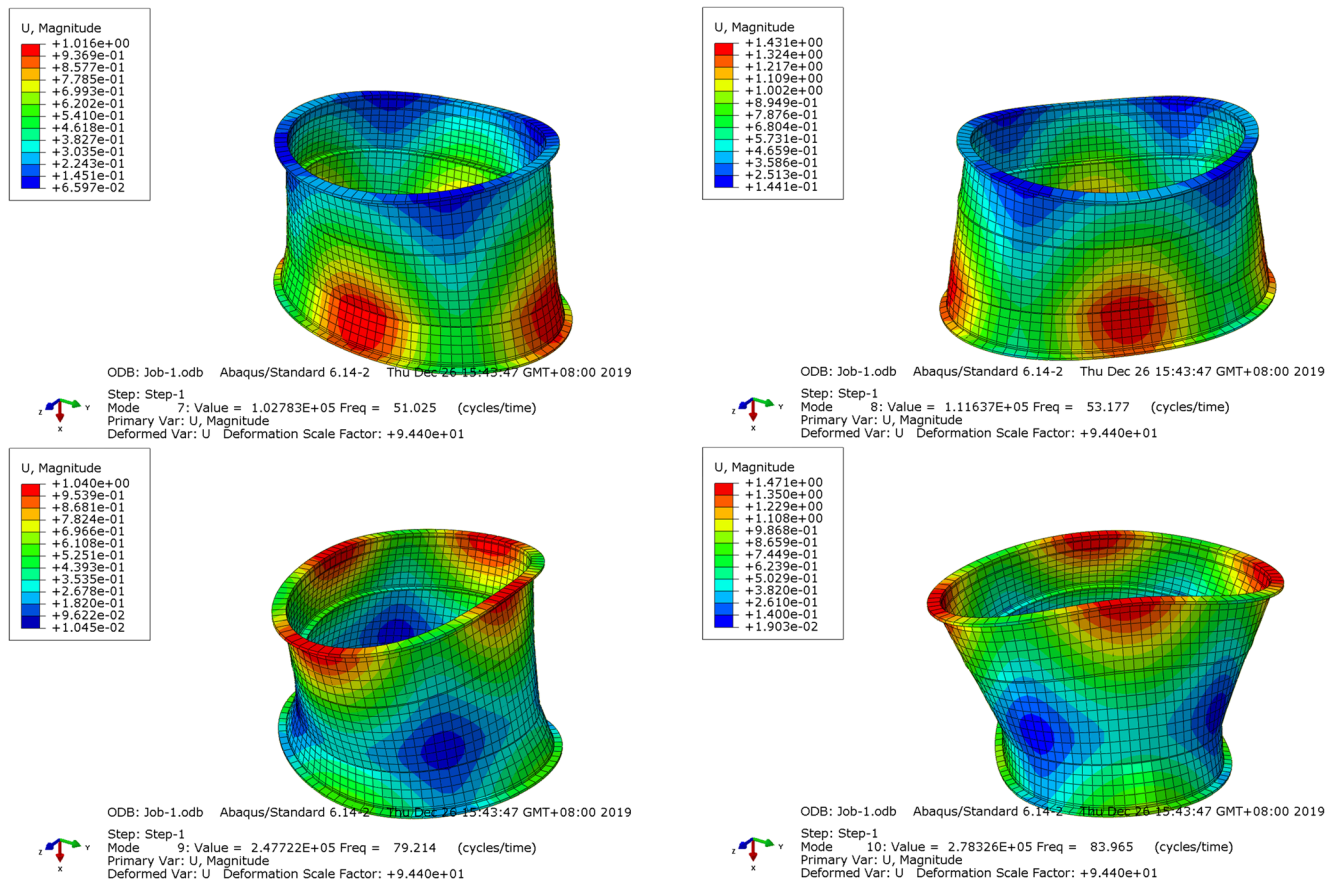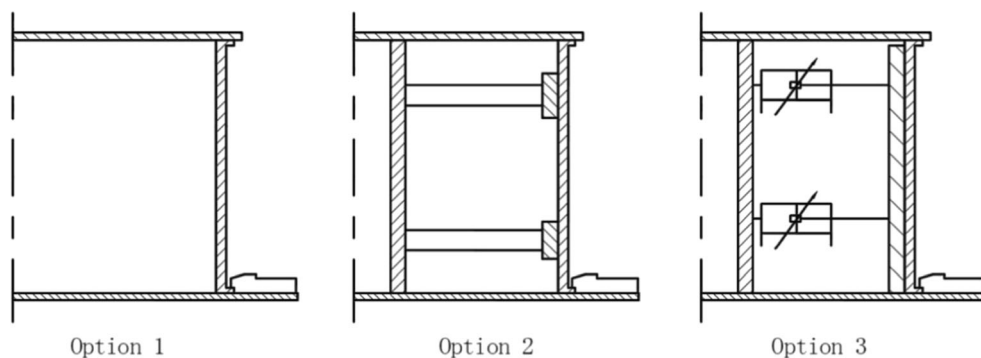

Fig. 5 Results of the 7th to 10th mode shapes

Fig. 6 Scheme of the clamping system

(pneumatic transmission). In order to facilitate the comparison of various schemes, option 1 of the clamping system without auxiliary support is added as a reference.

In ABAQUS, a finite element model including a clamping system and a casing is established for the three milling and clamping schemes of the simplified casing parts shown in Fig. 4-b, and then a constraint modal analysis is performed. The constraints of the three milling and clamping systems are shown in Table 2:

After ABAQUS finite element constraint modal analysis, the analysis results are shown in Fig. 7. Intersect the natural frequencies of the 1st to 10th order of the three milling clamping systems with the part-machine-tool system resonance interval (250 Hz ~ 650 Hz). The probability of resonance which may occur without auxiliary support is 100%, and the multi-point rigid auxiliary support is 67.63%. The auxiliary support of the flexible surface is 24.27%. From this analysis, it can be obtained that the flexible surface auxiliary support has the largest impact on the dynamic performance of the casing structure. It can be inferred that in theory, the third solution will have the most significant effect on milling vibration suppression.

3.2.2 Constrained modal analysis based on physical experiments

In order to verify the correctness of the abovementioned finite element-based constrained modal analysis, it also laid the foundation for the later finite element-based harmonic response analysis. Constrained modal analysis was performed using the casing parts shown in Fig. 4-a as experimental

objects, and corresponding physical test experiments were carried out. The experiment consists of three parts: a test system, signal acquisition, and analysis system, and a data processing and analysis system. The test system includes the casing, fixture, acceleration sensor, and force hammer. The signal acquisition and analysis software is the Cutpro MaLT module, and the data processing and analysis software is Utekl spectrum analysis software. The constrained modal results of the three clamping schemes of the part were measured by the hammer method, and the result data was compared with the modal analysis based on the finite element method. The specific experimental process is shown in Fig. 8:

From the results of finite element simulation and physical experiment modal analysis in Table 3, it can be seen that the natural frequency of the flexible surface auxiliary support scheme has been improved, avoiding the natural frequency range of most machine tools and reducing the possibility of resonance. At the same time, the comparison between the simulation data and the data of the physical experiment results shows that the error is mostly kept at about 20%, which indicates that the results of the constraint modal analysis based on the finite element method are reliable. From this experiment, it can be seen that the clamping scheme using the flexible surface auxiliary support has the best effect on improving the natural frequency of the system to be processed including the casing, and avoids most of the resonance interval.

In order to further verify the vibration reduction effect of the flexible surface auxiliary support clamping system, a set of multi-point rigid auxiliary supports and flexible surface

Table 2 Constraints for milling fixture systems

Program	Restrictions	Exposure
Without auxiliary support	The bottom edge of the casing is fixed and restrained	No
Multi-point rigid auxiliary support	The bottom edge of the casing is fixed and restrained; The inner wall is radially rigidly supported.	Multi-point surface contact
Flexible surface support	The bottom edge of the casing is fixed and restrained; The inner wall is radially supported flexibly.	Cylindrical surface contact

Fig. 7 Three support fixture restraint modes
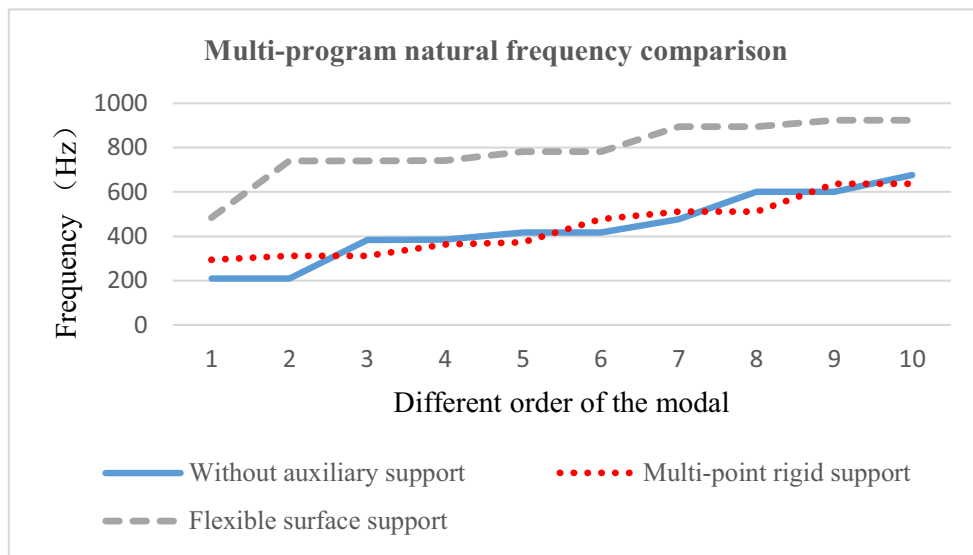
supports will be used to simulate the harmonic response comparison simulation experiments.

4 Harmonic response analysis based on finite element simulation

4.1 Comparison of harmonic response between multi-point support and flexible surface support

Based on the abovementioned simulation system, a dynamic response force of 400 N in the X / Y / Z direction is applied to the center point of the tool. The frequency range of the harmonic force is set to 0 Hz to 1500 Hz according to the modal analysis result, and the number of substeps is taken to be 200. At the same time, the 6 degrees of freedom of the casing is completely restricted. The maximum amplitude is used to evaluate the vibration reduction effect of the two solutions of rigid support and flexible surface support.

The finite element simulation of the flexible surface auxiliary support involves the relevant damping coefficients. Therefore, the system damping ratio of the fixture system is measured by the hammer method, and the damping ratio of the fixture system is 10.94%. The simulation analysis results of

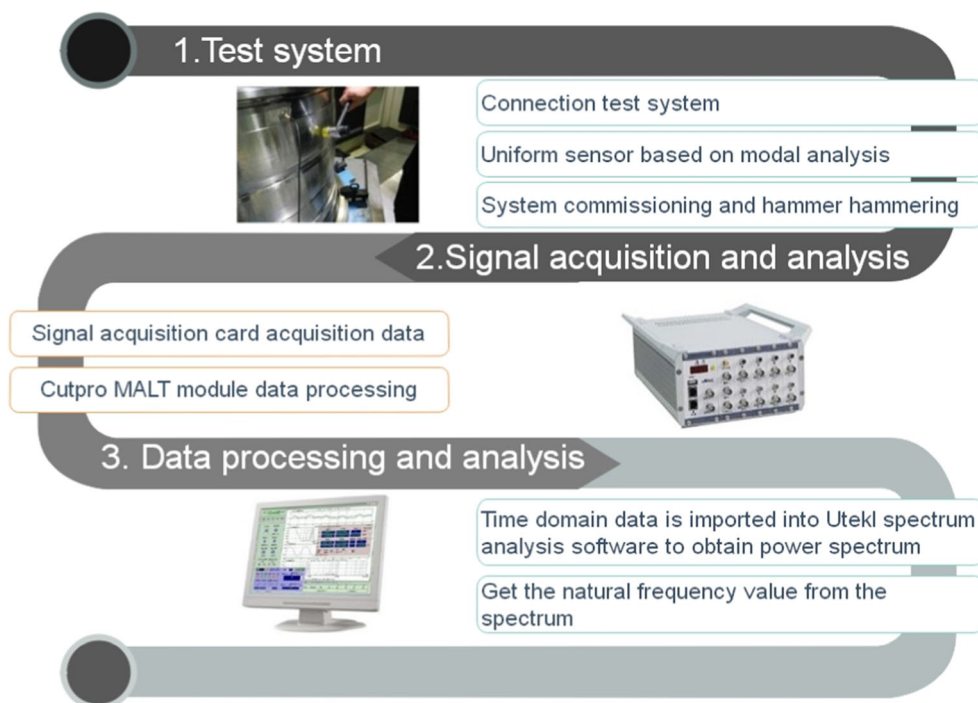**Fig. 8** Natural frequency of the hammer test system

Table 3 Natural frequency comparison

Order	Modal(Hz)								
	Without auxiliary support			Multi-point rigid auxiliary support			Flexible surface support		
	Physics experiment	Finite element simulation	error	Physics experiment	Finite element simulation	error	Physics experiment	Finite element simulation	error
1	179.94	209.07	16.19%	370.21	294.01	20.58%	408.850	483.95	15.52%
2	180.51	209.07	15.82%	371.7	312.28	15.98%	456.810	739.09	38.19%
3	347.16	383.02	10.33%	431.36	312.29	27.60%	586.740	739.13	20.62%
4	349.71	384.49	9.95%	466.15	362.99	22.13%	768.800	741.45	3.69%
5	516.68	417.82	19.13%	485.65	372.19	23.36%	816.760	782.27	4.41%
6	523.15	417.92	20.11%	488.73	477.07	2.39%	1031.000	782.32	31.79%
7	525.11	477.07	9.15%	490.66	511.42	4.23%	1070.700	894.18	19.74%
8	528.62	599.95	13.49%	633.94	511.43	19.33%	1071.100	894.81	19.70%
9	532.75	599.95	12.61%	637.06	637.03	0.000047%	1100.600	922.53	19.30%
10	646.9	676.93	4.64%	784.35	637.19	18.76%	1168.800	922.53	26.70%

the harmonic response of the simulation process are shown in Fig. 9. From the simulation results, it can be seen that the vibration deformation of the multi-point rigid auxiliary support clamping system reaches a maximum value of 0.122 mm at 329.6 Hz, and the maximum deformation occurs in the unsupported part through the deformation cloud diagram. The flexible surface auxiliary support clamping system achieves a maximum of 0.005 mm at 795.7 Hz, and the vibration reduction effect is as high as about 90%.

From this comparison experiment, it can be seen that the vibration reduction effect of the flexible surface auxiliary support clamping system is significantly better than that of the multi-point rigid auxiliary support clamping system. Next, a full factor experimental study is performed on the factors affecting the vibration deformation of the flexible surface auxiliary support clamping system.

4.2 Multi-factor harmonic response analysis of flexible surface support

Air pressure is the most important variable factor of the flexible surface auxiliary support fixture system. The main influencing factor of the machining system on the milling process is the milling force, and the changing factors of the casing parts include the diameter, case thickness, and material type. For the Rolls-Royce aeroengine combustor casing, precipitation-enhanced nickel-based superalloy GH4169 is mostly used. Therefore, the diameter, case thickness, milling force, and support pressure of the casing parts are the main analysis objects. The sreacheteady-state dynamics module based on the modal analysis in ABAQUS linear perturbation is used to analyse the harmonic response of the part to simulate the effect of different working conditions and part

Fig. 9 Comparison of harmonic response between point support and flexible surface support
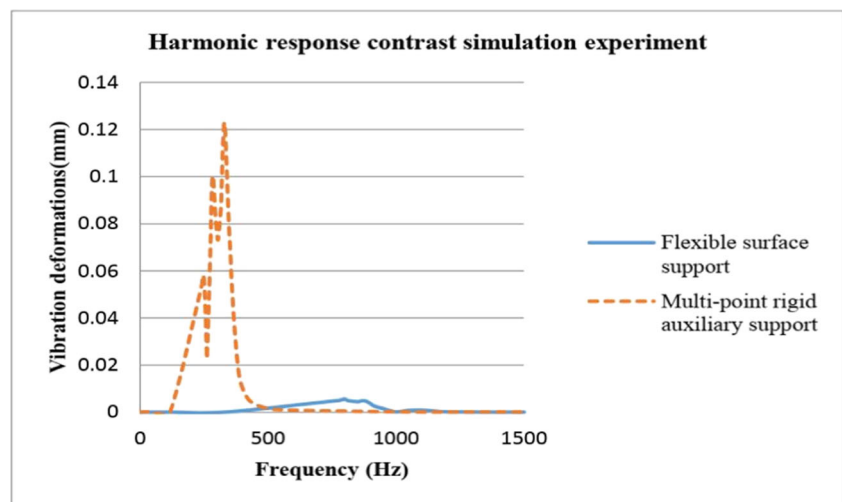
Table 4 Experimental parameters (1)

	Diameter(mm)		Case thickness(mm)	Milling force(N)	Support pressure(bar)
	The inner diameter of the casing	Support block diameter			
Group 1	800	660~800	3	200	0.12
Group 2	1000	860~1000	4	300	0.48
Group 3	1200	1060~1200	5	400	0.96

parameters on machining vibration. Based on the abovementioned preliminary preparation of the function shown in Formula 1, the exact functional relationship between each variable and the vibration deformation A is solved after the full-factor harmonic response simulation analysis.

$$A = f\ (F, r, p, b\ldots) \tag{1}$$

where A is the vibration deformation; F is the milling force; r is the diameter of the casing; p is the support pressure; and b is the thickness of the casing.

4.2.1 Full factor experiment

When the diameter of the casing parts is different, the corresponding supporting element size also changes. Combined with the parameters of various types of casings processed on-site, the specific parameters of all analysis factors are shown in Table 4. The material properties of the casing parts are the same as those in Table 1. The material of the support block is nylon. The material properties are as follows density: 1.13 g/cm^3, Young's modulus: 2620Mpa, Poisson's ratio: 0.34.

Using the multi-factor numerical range shown in Table 4 for the full factor 3^4 simulation experiment, a full factor experimental parameter table shown in Table 5 is constructed.

Process the simulation result data and fit the corresponding function relationship. First, a scatter plot is drawn for each influencing factor to predict the structural form of the function. The partial data scatter plot is shown in Fig. 10.

Then, use the data processing and analysis software SPSS to perform nonlinear regression analysis and function fitting of the data, and now obtain the following functional relationship:

$$y = (-0.149)x_0 + (0.011)x_1 + (-0.754)x_2$$
$$+ (1.636 \times 10^{-18})e^{0.033x_3} + 0.868 \tag{2}$$

where x_0 is the case thickness, x_1 is the milling force, x_2 is the support pressure, and x_3 is the diameter of the casing. According to formula 2, two conclusions can be obtained: (1) under the condition of flexible surface auxiliary support, the diameter of the casing has little effect on milling vibration, which can be almost ignored; (2) The relationship between case thickness, milling force, support air pressure, and vibration deformation amplitude are all linear. There are two reasons to explain this situation: 1. The range of influencing factors is too small; 2. The influencing factors are indeed linearly related to the amplitude of vibration deformation. Therefore, the full-factor experiment after the second optimization is extended. The analysis objects only include case thickness, milling force, and support air pressure, and the value interval of each influencing factor is expanded.

4.2.2 Optimised full factor experiment

The second full factor 4^3 simulation experiment was performed using the multi-factor numerical range shown in

Table 5 Full factor experimental parameter(1)

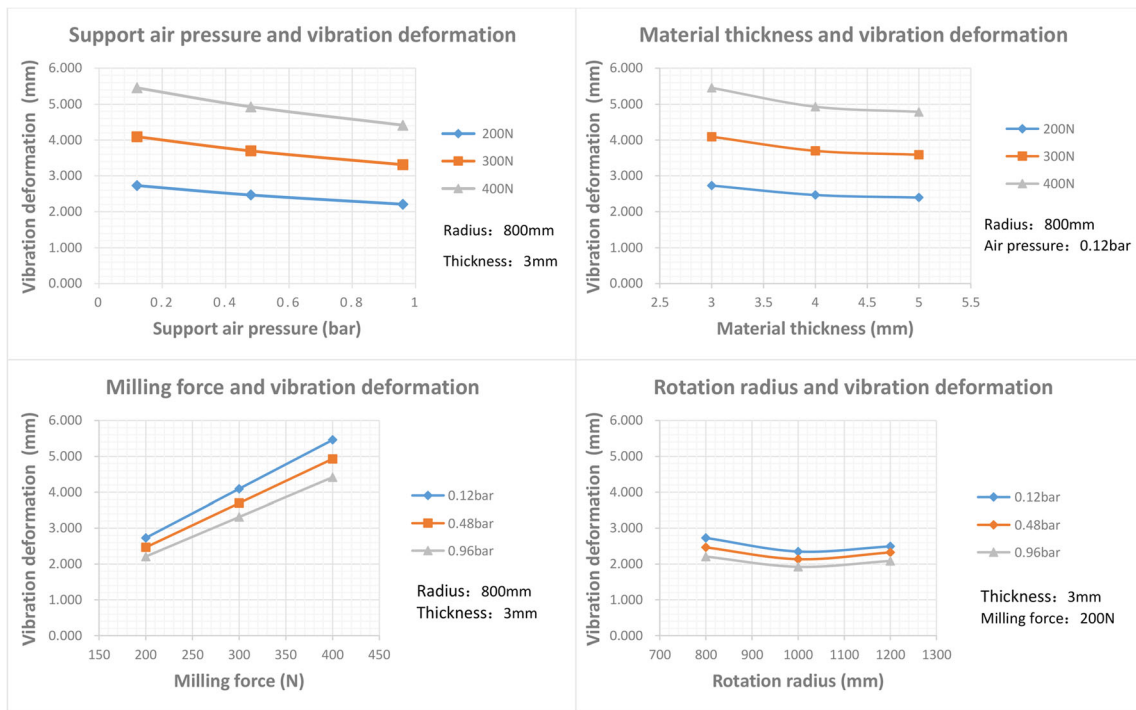|	Diameter(mm)	Case thickness(mm)	Milling force(N)	Support pressure(bar)
1	800	3	200	0.12
2	800	3	200	0.48
3	800	3	200	0.96
…	…	…	…	…
79	1200	5	400	0.12
80	1200	5	400	0.48
81	1200	5	400	0.96

Fig. 10 Full factor experimental scatter plot (partial)

Table 6 and the full factor experimental parameter table shown in Table 7 was constructed. Other parameters: diameter 800 mm, height 600 mm, casing and nylon material parameters are the same as those of the previous full factor experiment.

The nonlinear regression function in the SPSS software analysis module was used to perform limited nonlinear regression analysis on 64 sets of simulation result data. Set the vibration deformation as the dependent variable and construct a similar model expression based on the scatter plot of the second full factor experiment result, and find the optimal solution after 32 iterations:

$$y = 0.008x_1 + \frac{5.113}{0.898x_2} - 0.101x_2 + 0.846$$
$$\times\ 0.033^{x_3} - 0.656_{x_3} + 0.826 \tag{3}$$

where y is vibration deformation, x_1 is milling force, x_2 is the case thickness, and x_3 is supporting air pressure. As shown in Table 8, the square of the fitting function R reaches 0.912, indicating that the fitting regression effect is better.

5 Structural rigidity analysis based on static load experiment

In order to verify that the flexible surface-assisted support and clamping scheme can improve the radial rigidity of the casing, a static load experiment was carried out in this paper. This experiment can more directly express the effect of improving the rigidity of the system to be processed. The physical experiment environment is shown in Fig. 11.

A static load experiment was performed after using this type of combustion chamber casing with a flexible surface to support the clamping system. Different support air pressure conditions were set, a point load $F = 300\ N$ was applied to the surface at the middle height of the part, and the static deviation was measured at the same point, to identify the support rigidity of the system to be processed composed of different support pressures. The experimental

Table 6 Table of experimental parameters (2)

	Case thickness(mm)	Milling force(N)	Support pressure(bar)
Group 1	3	200	0.2
Group 2	5	400	0.6
Group 3	8	600	1.8
Group 4	12	800	5.4

Table 7 Full factor experiment parameter Table (2)

	Case thickness(mm)	Milling force(N)	Support pressure(bar)
1	3	200	0.2
2	3	200	0.6
3	3	200	1.8
…	…	…	…
62	12	800	0.6
63	12	800	1.8
64	12	800	5.4

Table 8 Variance analysis

ANOVA[a]

Source	Sum of squares	Degrees of freedom	Mean square
Regression	1431.327	8	178.916
Residual	37.697	56	0.673
Total before correction	1469.025	64	
Revised total	430.374	63	

Dependent variable: vibration deformation [a]

a. R = 1-(Residual sum of squares) / (Modified sum of squares) = 0.912。

results are shown in Fig. 12. Under the same static load, as the support pressure increases, the displacement of the casing surface gradually decreases.

The static load and displacement are substituted into the formula $F = kx$, and the stiffness coefficient corresponding to each support air pressure is obtained. The results are shown in Table 9.

A scatter plot of support pressure and stiffness coefficient is drawn from Table 9. Based on the scatter plot, a similar function model is constructed and the functional relationship between support pressure and stiffness coefficient is fitted: $K = 99.48e^{0.6229p} + 4.759$. The results show that the stiffness

coefficient of the structure increases exponentially with the increasing support pressure.

6 Conclusions

The machining quality of aeroengine casing parts is an important basis for the reliability, safety and high performance of an engine, but severe vibration during machining can cause severe tool wear. When the tool cannot withstand high cutting parameters, to reduce the production costs and meet the accuracy requirements for the part, one must reduce the cutting parameters. This leads to long processing cycles and low productivity. Therefore, suppressing the vibration of the casing during processing plays a vital role in cost control and production capacity improvements. To solve this problem, this paper first carries out a modal analysis of the casing parts to understand the deformation trend based on the finite element method, then designs a variety of matching clamping systems and compares the structural performance based on a combination of simulation experiments and physical experiments, uses the finite element simulation to simulate the machining environment, and builds a mathematical model of the optimal
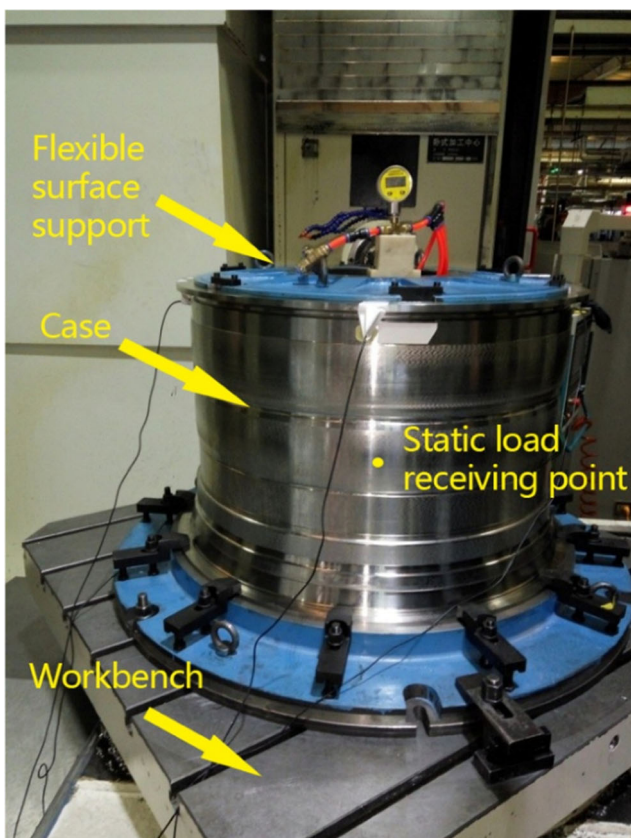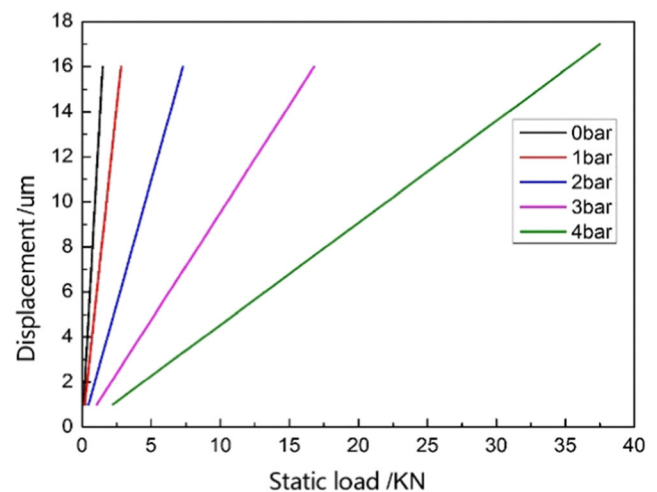

Fig. 11 Static load test

Fig. 12 Static load test results

Table 9 Support air pressure and stiffness coefficient

Air pressure(Bar)	Stiffness coefficient(Kn/mm)
0.0.	$k0 = \sum \frac{F}{X} = 112.4$Kn/mm
1.0	$k1 = \sum \frac{F}{X} = 175.6$Kn/mm
2.0	$k2 = \sum \frac{F}{X} = 356.6$Kn/mm
3.0	$k3 = \sum \frac{F}{X} = 650.1$Kn/mm
4.0	$k4 = \sum \frac{F}{X} = 1205.5$Kn/mm

support pressure and vibration deformation required for the processing of different types of casings. Finally, a static load experiment is carried out for the optimal scheme (flexible surface auxiliary support). The following conclusions are reached:

(1) Three matching clamping processing schemes are proposed, namely, no auxiliary support fixture, multipoint rigid auxiliary support, and flexible surface auxiliary support. The modal analysis results of the three clamping schemes show that the flexible surface auxiliary support increases the rigidity of the system to be processed while increasing the natural frequency of the system and avoiding the resonance interval with the tool system. Therefore, the flexible surface auxiliary support clamping system is the optimal solution.

(2) After a full factor experiment and the optimised full-factor simulation experiments, the functional relationship between the case thickness, support air pressure, milling force, and vibration deformation of the casing and the trend of its influence is successfully fitted, and the fitted function R square reaches 0.912. This function can match the optimal support air pressure and vibration deformation prediction for different casing parts during field processing.

(3) A structural rigidity analysis based on static load experiments shows that the air pressure-assisted support scheme has an excellent improvement effect on the structural rigidity of the processing system. With the continuous increase in the support pressure, the structural rigidity of the system to be processed is increased exponentially.

Aeroengine casing milling vibration suppression is of great significance in high-efficiency, high-quality and high-precision machining. In this study, a set of methods for suppressing the milling vibration of a casing is proposed, which provides technical guidance for production and improves the processing quality and efficiency of the casing, which has very important engineering value and economic benefits. Next, multiple sets of casing milling fixtures will be designed based on the flexible auxiliary surface support clamping

scheme, vibration deformation will be detected, and the optimal air pressure support will be adjusted during on-site processing. The results will be used to verify and improve the mathematical model of vibration deformation.

Authors' contributions Liang Guo is responsible for paper conception.
Fan Yang is responsible for experimental design.
Tian Li is responsible for experimental data analysis.
Ming Zhou is responsible for the installation of experimental equipment.
Junlei Tang is responsible for experimental summary.

Data availability The datasets used or analysed during the current study are available from the corresponding author on reasonable request.

Compliance with ethical standards

Ethical approval Not applicable

Consent to participate Yes

Consent to publish Yes

Conflict of interest The authors declare that they have no conflict of interest.

References

1. Wan M, Gao T, Feng J, Zhang W (2019) On improving chatter stability of thin-wall milling by prestressing. J Mater Process Technol 264:32–44. https://doi.org/10.1016/j.jmatprotec.2018.08.042
2. Wan S, Li X, Su W, Yuan J, Hong J, Jin X (2019) Active damping of milling chatter vibration via a novel spindle system with an integrated electromagnetic actuator. Precis Eng 57:203–210. https://doi.org/10.1016/j.precisioneng.2019.04.007
3. YUE C, GAO H, LIU X, LIANG SY, WANG L (2019) A review of chatter vibration research in milling. Chin J Aeronaut 32:215–242. https://doi.org/10.1016/j.cja.2018.11.007
4. Wenxi L, Qidou Z (2019) Vibration characteristics of cylindrical shells with unevenly arranged ribs. Ship Mech 23:68–77
5. Bolar G, Das A, Joshi SN (2018) Measurement and analysis of cutting force and product surface quality during end-milling of thin-wall components. Measurement 121:190–204. https://doi.org/10.1016/j.measurement.2018.02.015
6. Min F, Zhu X, Tianyun L, Hu X (2018) An analytical method for free vibration analysis of ring-ribbed elliptic cylindrical shells. Vib Shock 37:138–146
7. Wang S, Jia Z, Lu X, Zhang H, Zhang C, Liang SY (2018) Simultaneous optimization of fixture and cutting parameters of thin-walled workpieces based on particle swarm optimization

algorithm. Simul Trans Soc Model Simul Int 94. https://doi.org/10.1177/0037549717713850

8. Wang M, Zhaobo C, Yinghou J, Lu W (2017) Vibration characteristics of thin-walled cylindrical shells with constrained damping. J Harbin Inst Technol 49:72–79

9. Zhang FP, Yan Y, Butt SI (2016) Integrated model based thin-walled part machining precision control for the workpiece-fixture system. Int J Adv Manuf Technol 85:1745–1758. https://doi.org/10.1007/s00170-015-8036-8

10. Lu T, Gang J, Qidou Z, Weikang Z, Wenxi L (2017) Effect of equidistant arrangement of structures on the vibration performance of cylindrical shell structures. J Vib Eng 30:603–609

11. Munoa J, Beudaert X, Dombovari Z, Altintas Y, Budak E, Brecher C, Stepan G (2016) Chatter suppression techniques in metal cutting. CIRP Ann 65:785–808. https://doi.org/10.1016/j.cirp.2016.06.004

12. Yu W, Luo Z (2015) Research on the response characteristics of thin-walled cylindrical shell members subjected to forced vibration. Vib Shock 34:103–108

13. Kolluru K, Axinte D (2013) Coupled interaction of dynamic responses of tool and workpiece in thin wall milling. J Mater Process Technol 213:1565–1574. https://doi.org/10.1016/j.jmatprotec.2013.03.018

14. By Tang ATA, Liu ZLZ (2008) Deformations of thin-walled plate due to static end milling force. J Mater Process Technol:345–351. https://doi.org/10.1016/j.jmatprotec.2007.12.089

15. Siebenaler SP, Melkote SN (2006) Prediction of workpiece deformation in a fixture system using the finite element method. Int J Mach Tools Manuf 46:51–58. https://doi.org/10.1016/j.ijmachtools.2005.04.007

16. Fei J, Lin B, Xiao J, Ding M, Yan S, Zhang X, Zhang J (2018) Investigation of moving fixture on deformation suppression during milling process of thin-walled structures. J Manuf Process 32:403–411. https://doi.org/10.1016/j.jmapro.2018.03.011

17. Do MD, Son Y, Choi H (2018) Optimal workpiece positioning in flexible fixtures for thin-walled components. Comput Aided Des 95:14–23. https://doi.org/10.1016/j.cad.2017.09.002

18. Sallese L, Innocenti G, Grossi N, Scippa A, Flores R, Basso M, Campatelli G (2017) Mitigation of chatter instabilities in milling using an active fixture with a novel control strategy. Int J Adv Manuf Technol:2771–2787. https://doi.org/10.1007/s00170-016-9831-6

19. Qin G, Wang Z, Rong Y, Li Q (2017) A unified approach to multi-fixturing layout planning for thin-walled workpiece. Proc Inst Mech Eng B J Eng Manuf 231:454–469. https://doi.org/10.1177/0954405415585240

20. Ma J, Zhang D, Wu B, Luo M, Liu Y (2017) Stability improvement and vibration suppression of the thin-walled workpiece in milling process via magnetorheological fluid flexible fixture. Int J Adv Manuf Technol 88:1231–1242. https://doi.org/10.1007/s00170-016-8833-8

21. Ma J, Zhang D, Wu B, Luo M, Chen B (2016) Vibration suppression of thin-walled workpiece machining considering external damping properties based on magnetorheological fluids flexible fixture. Chin J Aeronaut 29:1074–1083. https://doi.org/10.1016/j.cja.2016.04.017

22. Wang T, Zha J, Jia Q, Chen Y (2016) Application of low-melting alloy in the fixture for machining aeronautical thin-walled component. Int J Adv Manuf Technol 87:2797–2807. https://doi.org/10.1007/s00170-016-8654-9

23. Wan X, Zhang Y, Huang X (2013) Investigation of influence of fixture layout on dynamic response of thin-wall multi-framed workpiece in machining. Int J Mach Tool Manu 75:87–99. https://doi.org/10.1016/j.ijmachtools.2013.09.008

24. Jiang X, Zhao G, Lu W (2020) Vibration suppression of complex thin-walled workpiece based on magnetorheological fixture. Int J Adv Manuf Technol 106:1043–1055. https://doi.org/10.1007/s00170-019-04612-2

25. Yang Y, Xu D, Liu Q (2014) Vibration Suppression of Thin-Walled Workpiece Machining Based on Electromagnetic Induction. Mater Manuf Process 30:829–835. https://doi.org/10.1080/10426914.2014.962042

26. Kolluru K, Axinte D (2014) Novel ancillary device for minimising machining vibrations in thin wall assemblies. Int J Mach Tools Manuf 85:79–86. https://doi.org/10.1016/j.ijmachtools.2014.05.007

27. Kolluru KV, Axinte DA, Raffles MH, Becker AA (2014) Vibration suppression and coupled interaction study in milling of thin wall casings in the presence of tuned mass dampers. Proc Inst Mech Eng B J Eng Manuf 228:826–836. https://doi.org/10.1177/0954405413508769

28. Kolluru K, Axinte D, Becker A (2013) A solution for minimising vibrations in milling of thin walled casings by applying dampers to workpiece surface. CIRP Ann 62:415–418. https://doi.org/10.1016/j.cirp.2013.03.136

29. Zeng S, Wan X, Li W, Yin Z, Xiong Y (2012) A novel approach to fixture design on suppressing machining vibration of flexible workpiece(Article). Int J Mach Tools Manuf:29–43. https://doi.org/10.1016/j.ijmachtools.2012.02.008

30. Wang X, Song Z, Xiujie J (2011) Optimization of aero-engine integral casing milling-turning composite machining process. Comput Integr Manuf Syst 17:1460–1465

Publisher's note Springer Nature remains neutral with regard to jurisdictional claims in published maps and institutional affiliations.